Constitutive modeling and Computational Simulations of the external pressure induced buckling collapse of High Density Polyethylene (HDPE) liners

Patricia M. Frontini[1,*], **Federico Rueda**[1], **Juan P. Torres**[2]

[1] Instituto de Tecnología y Ciencia de Materiales, Universidad Nacional de Mar del Plata, B7608FDQ, Argentina
* Corresponding author: pmfronti@fi.mdp.edu.ar

Abstract The objective of this work is to evaluate the capability of an advanced constitutive model, namely the Three Network Model (TNM) of simulating the mechanical response of HDPE liners undergoing buckling collapse. In order to determine the input parameters for the model, a series of tensile and compressive uniaxial tests were conducted. Simulations were performed using Finite element modeling (FEM) analysis with the ABAQUS 6.10 package. The complex strain rate, temperature and pressure dependent mechanical response of HDPE was analyzed by modeling the dynamic event as an increasing volume of fluid entering the gap cavity between liner and host pipe, and a mathematical relationship between fluid flow rate and collapse pressure was proposed.

Keywords buckling collapse, constitutive modeling, HDPE liners, Finite Element modeling

1. Introduction

The use of polymers in the gas and oil transportation industry is nowadays widely spread. One of their main uses is as lining materials for oil and gas pipelines. These liners serve the function of providing internal protection of metallic tubes mainly in two different situations, namely: by providing enhanced corrosion resistance from aggressive chemical agents, and, in a rehabilitation technique for damage pipes known as relining, during which these structures are slip lined with a polyethylene liner that replaces the inoperative section of the tube [1]. However, there is a number of ways in which polymeric liners can fail in service after a certain time. The present study specifically concerns with the buckling collapse of liners induced by external pressure. This failure mode takes place by the combined action of two separate factors, these are: *i)* the permeation of oil derived gases through the liner wall for extended periods of time, and *ii)* the rapid decompression of pipelines that can occur during service stoppages or maintenance and inspection shutdowns [2].

Recently, a number of studies have been devoted to understand the underlying mechanisms that eventually lead to liner failure [3,4]. Material failure is associated with the phenomenon known as physical swelling. This occurs in liners when some organic components, such as the CO_2 and CH_4 dissolved in oil, penetrate into the polymer macromolecular chain network aided by the high pressure operating conditions, increasing the space between molecules and decreasing the intermolecular bonding. As this operation takes place, the migratory gases can permeate throughout the liner wall and gradually balance the pressure difference between the inside of the liner and the annular region consisting of the gap between the liner and the pipe wall. This permeation mechanism worsens recursively since permeation rate increases with the severity of swelling of the liner. Finally, buckling collapse occurs when the liner is intentionally decompressed and the external pressure built up by the confined gases in the annular region, generates a stress state in the liner that induces the radial buckling failure.

Currently, a number of analytical models that deal with the buckling collapse of metallic tubes under external pressure have been developed in the literature [5-7]. In all cases, the analytical solutions found are restricted to purely elastic or ideal elastoplastic behavior and cannot analyze the influence of geometrical or surface defects, so commonly generated during the manufacturing, storage, transport and installation stages. Moreover, they are only useful for obtaining a critical

pressure value and are not able to describe the whole deformation process. On the other hand, in [8], Rueda et al. developed a specific FEM model for the simulation of the buckling collapse of HDPE liners. In their work, they were able to simulate an overall buckling collapse situation by introducing hydrostatic fluid elements in the model to allow for hydraulic effects. For the description of material constitutive response, they used linear elastic, linear elastoplastic, and linear elastoplastic with strain hardening behavior. Their investigation served as the first step for the prediction of actual failure situations since it showed that the transient dynamic response could be effectively simulated by FEM analysis. However, the traditional constitutive models used in their work cannot account for the intrinsic strain-rate, pressure and temperature dependence of polymer mechanical behavior and therefore are not sufficient to reproduce the complex multiaxial stress response and rate-dependent deformation evolution that will take place during an actual rapid pipe depressurization situation. As a consequence, it remains to include into the analysis an advanced constitutive model capable of accounting for the intricate response of polymers.

Constitutive modeling of polymers is nowadays a well-established field with a large number of advances over the last 40 years. In this regard, one of the most successful developments has been the family of tridimensional constitutive models started by Boyce and coworkers [9-13], which brought together current theories of macromolecular physics with recent work in the fields of statistical mechanics, continuum mechanics, and computational mechanics. These models employ a constitutive framework intended to be general enough to capture material behavior over a wide range of loading conditions, in order to be appropriate for their use in FEM analysis. The original work of Boyce et al. [9] was concerned with the large viscoplastic deformation of amorphous polymers, such as polycarbonate (PC) and acrylic glass (PMMA). So far, this constitutive approach has been consecutively enhanced in order to include additional features of polymer deformation such as, strain induced anisotropy, rubber elasticity, thermo-mechanical coupling, high strain-rate testing and so on. Among these, a notable contribution was the Hybrid Model (HM) of Bergstrom et al. [14] which was designed for capturing the mechanical response of a semi-crystalline polymer: Ultra-high molecular weight polyethylene (UHMWPE). Following this, in [15], Bergstrom et al. developed the Three Network Model (TNM) which is a further refinement of the HM model to be more accurate and computationally efficient. For its pertinence regarding semi-crystalline thermoplastic polymers, the TNM model results in a suitable choice for modeling the mechanical response of HDPE liners. Therefore, the objective of the present work is the evaluation and validation of the TNM model, for its use in FEM assisted design to accurately predict the buckling failure in pipes in a varying range of temperature and loading-rate conditions.

2. Experimental

2.1. Uniaxial tensile and compression tests

For the calibration of the TNM material model, tensile and compression tests were performed on an Instron 4467 universal testing machine. Tensile and compression specimens were machined out from a supplied liner as indicated in Figure 1. In order to univocally determine the viscous parameters, the tests were carried out at 3 different strain-rates, corresponding to crosshead speeds of 1, 10 and 50 mm/min. Tensile tests were performed using a extensometer of 12.5mm gauge length. Compression tests were carried out employing specimens of approximately 10 mm in height and 5 mm in diameter according to 2:1 (height : diameter) ratio recommended in [16]. For a complete characterization of deformation evolution, both loading and unloading response was registered.

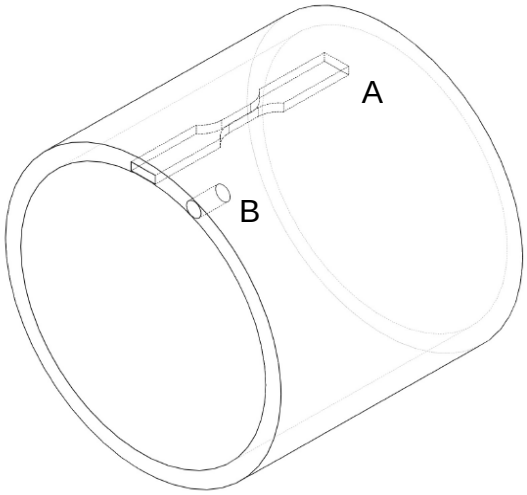

Figure 1. Tensile (A) and compression (B) specimens as obtained from the liner.

3. Computational efforts

3.1. Constitutive model

The main aspects of the TNM model constitutive framework will be described below, more details on the formulation can be found on the original works [14,15]. The TNM model consists of three networks acting in parallel as can be shown in the rheological representation (Fig.2)
The total deformation gradient of the assembly is decomposed into a thermal expansion component and a mechanical deformation component:

$$\mathbf{F}^{app} = \mathbf{F}\mathbf{F}^{th}$$

The mechanical deformation gradient of networks A and B are further decomposed into elastic and viscoplastic components:

$$\mathbf{F} = \mathbf{F}_n^e \mathbf{F}_n^v$$

Where *n* takes the value *A* and *B*, for networks *A* and *B* correspondingly. The Cauchy stress acting in networks A and B has the following form:

$$\boldsymbol{\sigma}_n = \frac{\mu_n}{J_n^e \overline{\lambda_n^{e*}}} \left[1 + \frac{\theta - \theta_0}{\hat{\theta}} \right] \frac{\mathcal{L}^{-1}\left(\overline{\lambda_n^{e*}} / \lambda_L \right)}{\mathcal{L}^{-1}\left(1/\lambda_L \right)} \mathrm{dev}\left[\mathbf{b}_n^{e*} \right] + \kappa \left(J_n^e - 1 \right) \mathbf{1}$$

Where, $J_n^e = \det[\mathbf{F}_n^e]$; $\mathbf{b}_n^{e*} = (J_n^e)^{-2/3} \mathbf{F}_n^e (\mathbf{F}_n^e)^{\mathrm{T}}$ is the Cauchy-Green deformation tensor; $\overline{\lambda}_n^{e*} = (\mathrm{tr}[\mathbf{b}_n^{e*}]/3)^{1/2}$ is the effective chain stretch and $\mathcal{L}^{-1}(x)$ is the inverse Langevin function.

The velocity gradient of networks A and B has the following form:

$$\dot{\mathbf{F}}_n = \dot{\chi}_n \mathbf{F}_n^{e-1} \frac{\mathrm{dev}[\boldsymbol{\sigma}_n]}{\tau_n} \mathbf{F}$$

Where:

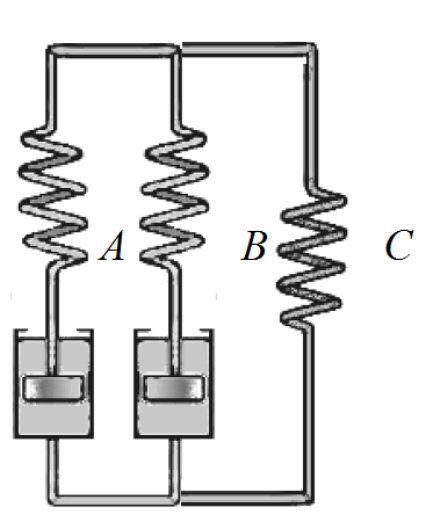

Figure 2. Rheological representation of the TNM constitutive model.

$$\dot{\gamma}_n = \dot{\gamma}_0 \left(\frac{\tau_n}{\hat{\tau}_n + aR(p_n)} \right)^{m_n} \left(\frac{\theta}{\theta_0} \right)^{n}$$

Here *R(x)* is the ramp function; p_n is the hydrostatic pressure; τ_n is the Fronebius norm of the deviatoric part of $\boldsymbol{\sigma}_n$.
The Cauchy stress acting in network C has the following form:

$$\boldsymbol{\sigma}_C = \frac{1}{1+q} \left\{ \frac{\mu_C}{J\lambda_{chain}} \left[1 + \frac{\theta - \theta_0}{\hat{\theta}} \right] \frac{\mathcal{L}^{-1}(\lambda_{chain}/\lambda_L)}{\mathcal{L}^{-1}(1/\lambda_L)} \mathrm{dev}\left[\mathbf{b}^* \right] + \kappa (J-1)\mathbf{1} + q \frac{\mu_C}{J} \left[I_1^* \mathbf{b}^* - \frac{2I_2^*}{3}\mathbf{I} - (\mathbf{b}^*)^2 \right] \right\}$$

Where $J = \det[\mathbf{F}]$; $\mathbf{b}^* = J^{-2/3}\mathbf{F}(\mathbf{F})^{\mathrm{T}}$ is the Cauchy-Green deformation tensor, and $\lambda_{chain} = (\mathrm{tr}[\mathbf{b}^*]/3)^{1/2}$
Finally, since they are in parallel, the three networks have equal mechanical deformation gradients and the total stress of the system is the sum of each network stress.

The TNM model was coded as a user material subroutine (UMAT/VUMAT) for ABAQUS and the constitutive parameters were determined using MCalibration software which uses a minimization algorithm based on the Nelder-Mead simplex method [17].

3.2. Liner-pipe system FEM model

The buckling collapse event was simplified assuming an ideal vacuum in the interior cavity of the liner and an increasing volume of fluid entering the liner-pipe cavity at a fluid flow rate *q*. This simplification has been made since this situation is easier to reproduce experimentally under controlled laboratory conditions. The event was simulated using ABAQUS/Implicit 6.10 for *q* values ranging from 10^{-5} to 10^{5} cm^3/s.

The thermoplastic liner was modeled as a planar bidimensional deformable solid (Fig.3a) using CPE8R elements and assuming plain strain, i.e. neglecting the effect of restraint at the liner ends. This assumption has proven to be valid for length to radius *L/R* values greater than 2 [18]. A small elliptical curvature was introduced in the upper part of the liner along the positive region of the

y-axis in order to induce single lob buckling (Fig.3b) in this region, which is the most critical failure mode and the most frequently observed in practice. Symmetry conditions were imposed with respect to the y-axis. The external metallic tube was assumed to be completely rigid in order to save CPU time. The fluid was modeled using F2D2 hydrostatic fluid elements and the depressurization event was modeled by imposing a fluid volume flux using the "fluid flux" option in ABAQUS/Implicit. These hydrostatic fluid elements are surface elements that cover the boundary of fluid containing cavity and provide the coupling between the deformation of the fluid-filled solid and the pressure exerted by the contained fluid on the solid surface defined as cavity boundary [19].

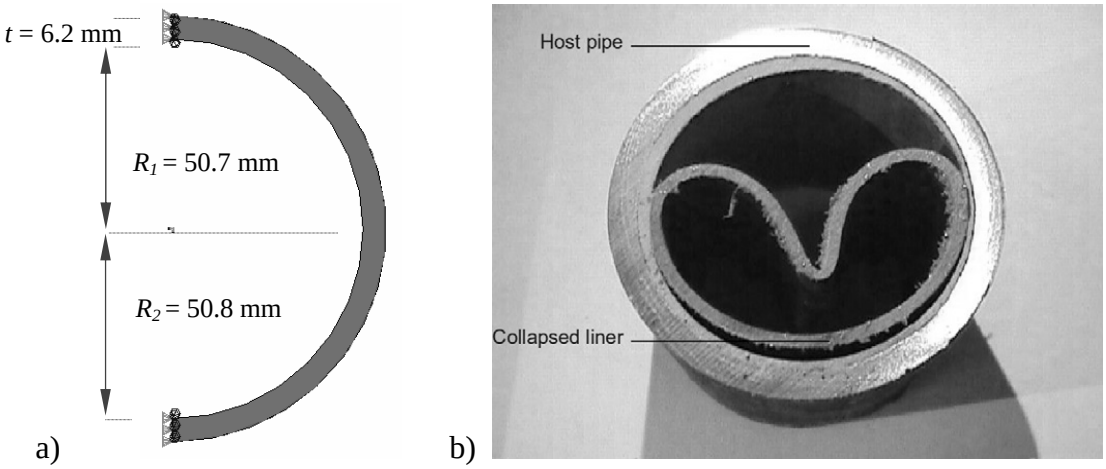

Figure 3. a) liner geometry and boundary conditions for the FEM model. b) single lob failure mode geometry

4. Results & Discussion

4.1. Uniaxial tensile and compression tests

Tensile and compression tests results are shown in Fig.5. In both cases, an initial time-independent elastic response can be observed. At a stress value of 5 MPa approximately the material enters the visco-elastoplastic regime, this region corresponds to the complex onset of different plastic flow mechanisms in the amorphous and semicrystalline domains of the thermoplastic material. In the constitutive model, the deformation gradients of the dashpots, which were at first negligible, start to flow at these stress values. Also in this regime, hardening is observed with increasing of strain rate, as expected. The material shows strain rate sensitivity both in tension and compression. Differences of approximately 30% in stresses are observed increasing 50 times the strain rate. Pressure dependency can be observed as the maximum stress achieved is higher in compression than in tension for equal deformation rates. A very good fit was obtained, with a R^2 (mean square difference) value of 1.5. The constitutive parameters obtained are presented in table 1.

4.1. FEM Simulations

Simulations predicted the buckling collapse pressure of the liner in all the range of q values. Fig 4 shows the final failure geometry in the simulations.

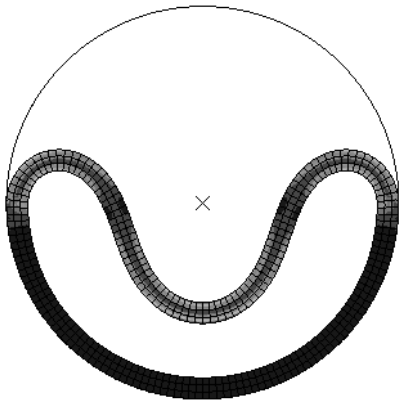

Figure 4. Final collapse geometry predicted by FEM simulations

Fig 6 shows the fluid pressure evolution as a function of fluid volume (V). Strain-rate dependency is manifested as it can be observed from the effect of increasing q values on fluid pressure, which are related to the speed at which the liner is accommodating deformation. Only at low values of V (up to V = 25 cm^3 approximately) a similar response can be observed for all q values, this is the initial elastic response which showed negligible strain-rate dependency as was noted in the tensile test results. In contrast, it can be seen that from V = 50 cm^3, higher q values lead to a more rapid increase in fluid pressure with fluid volume. This observation is consistent with the expected material stiffening as deformation rate increases (once in the visco-elastoplastic regime), meaning that, as the cavity is filled more rapidly, the liner can hold about the same volume of fluid at smaller deformations. This is done at the expense of the fluid high incompressibility, which therefore increases fluid pressure dramatically. Consequently, the maximum pressure attained, i.e. the collapse pressure, increases with q. Fig.7 shows the collapse pressure as a function of imposed flow rate. The logarithmic scale shows a potential relationship of the form $P_{max} = k.q^{RTF}$, where P_{max} is the collapse pressure, and *RTF* is a flow rate sensitivity exponent which ultimately characterizes the effect of material strain rate dependency on collapse pressure. The value of *RTF* is expected to be different for different materials, with *RTF* = 0 meaning a rate independent material. For the studied HDPE, the value of *RTF* obtained was approximately equal to 0.05. This factor can be of significant importance in the materials selection stage, when the values of expected depressurization velocities (v_{dep}) in service conditions are known. For this, a precise relationship between q and v_{dep} needs to be established. Furthermore, the possible influence of geometrical parameters such as the *t/D* ratio on the value of *RTF* still remains to be investigated.

Table 1. Constitutive parameters for the TNM model

Symbol	Name	Value
μ_A	Shear modulus of network A	40 MPa
λ_L	Chain locking stretch	1.02
$\hat{\theta}$	Temperature response of stiffness	-300 K
κ	Bulk modulus	2000 MPa
$\hat{\tau}_A$	Flow resistance of network A	2.07 MPa

a	Pressure dependence of flow	0.36
m_a	Stress exponential of network A	5.15
m_b	Stress exponential of network B	22.35
n	Viscosity parameter	40
$\hat{\tau}_B$	Flow resistance of network B	16.9 MPa
μ_{Bi}	Initial shear modulus of network B	259.3 MPa
μ_{Bf}	Final shear modulus of network B	60.51 MPa
μ_C	Shear modulus of network C	0.004 MPa
q	Relative contribution of I_2 of network C	zero

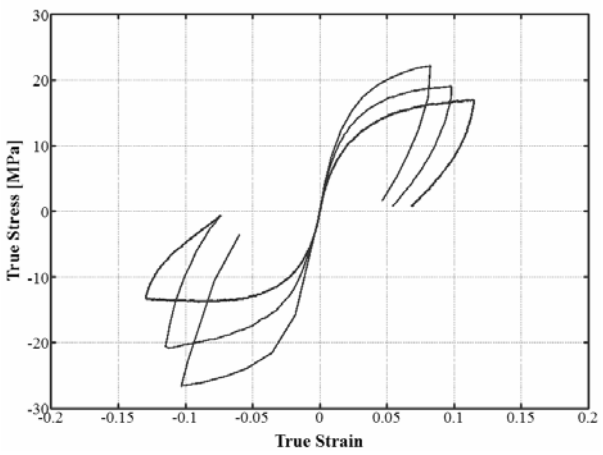

Figure 5. Uniaxial tensile and compression results at different cross-head speeds for HDPE.

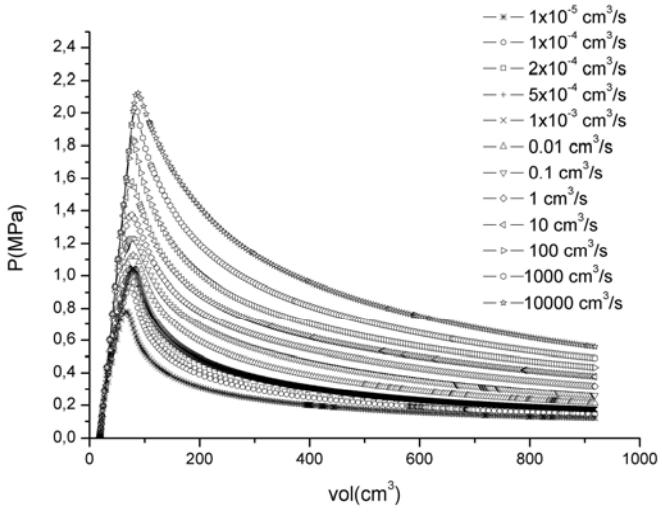

Figure 6. Evolution of fluid pressure, as a function of fluid volume in the liner-pipe cavity, for a wide range of fluid flow rates

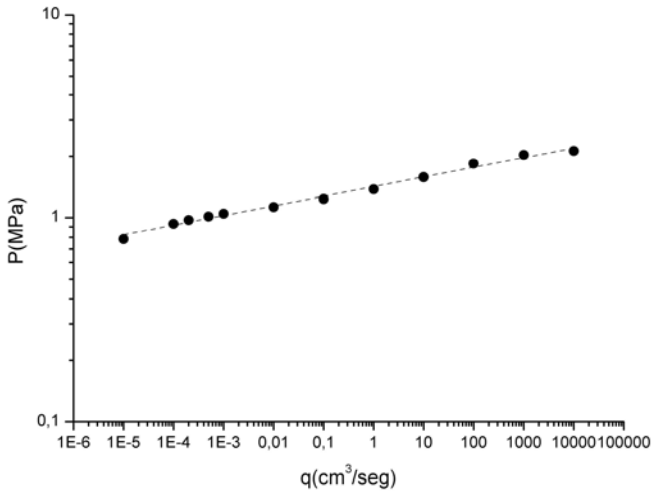

Figure 7. Collapse pressure as a function of imposed fluid flow rate.

5. Conclusion and forthcoming work

The external pressure-induced buckling collapse of thermoplastic liners was simulated using FEM analysis. The stress-strain response of the material and its intrinsic strain-rate and pressure dependency was modeled with the advanced TNM viscoelastic-viscoplastic model. Constitutive parameters were determined from tensile and compression stress-strain curves at different strain rates. The buckling failure event was simulated for a wide range of fluid flow rates. It was found that the material strain rate dependency has a significant effect on the collapse pressure P_{max} which leads to a potential relationship between P_{max} and q quantified by an exponent factor *RTF.* The value of *RTF* will vary with each material and quantifies the effect of strain rate dependency of the material on failure pressure. A forthcoming investigation will deepen the understanding of this factor and its dependence with the liner-pipe geometry. It also remains as future work to evaluate the prediction capability of the TNM model by comparing P_{max} FEM obtained values to empirical values determined under a controlled experimental setup.

References

[1] E. Engle, HR-370 Pipe rehabilitation with polyethylene pipe liners, 2003.
[2] Canadian Standards Association. CSA Z662-03 Oil and gas pipeline systems, 2003.
[3] B. Daniel, B.P. Lebsack, D.E. Hawn, R. Egner, Extending Liner Installation Lengths. United Pipeline Systems Inc., Corrosion, 2004 .
[4] NACE, RP0304-2004 liners for oilfield pipelines, 2004.
[5] D. Glock, Behavior of liners for rigid pipeline under external water pressure and thermal expansion. Der Stahlbau, 1977, pp. 212–217.
[6] S. Jacobsen, Buckling of circular rings and cylindrical tubes under external pressure. Water Power, 1974.
[7] KM. El-Sawy, Inelastic stability of tightly fitted cylindrical liners subjected to external uniform pressure. International Journal of Thin-Walled Structtures, 2001, pp.731–744.

[8] F. Rueda, J.L. Otegui, P.M. Frontini, Numerical tool to model collapse of polymeric liners in pipelines. Engineering Failure Analysis, 2011, pp. 24-34.
[9] M.C.Boyce, D.M. Parks, A.S. Argon, Large Inelastic Deformation of Glassy Polymers, Part I: Rate-Dependent Constitutive Model, Mechanics of Materials, 1988, pp. 15-33.
[10] E. M. Arruda, M. C. Boyce, A three-dimensional constitutive model for the large stretch behavior of rubber elastic materials, J. Mech. Phys. Solids. 1993, pp. 389–412.
[11] E. Arruda, M. Boyce, Effects of strain rate, temperature and thermo-mechanical coupling on the finite strain deformation of glassy polymers. Mech. Mater. 1995, pp. 193–212.
[12] J. S. Bergström, M. C. Boyce, Constitutive modeling of the large strain time-dependent behavior of elastomers. J. Mech. Phys. Solids, 1998, pp. 931–954.
[13] J. S. Bergström, M. C. Boyce, Large strain time-dependent behavior of filled elastomers, Mechanics of Materials, 2000, pp. 620–644.
[14] J. S. Bergström, C.M. Rimnac, S.M. Kurtz, An augmented hybrid constitutive model for simulation of unloading and cyclic loading behavior of conventional and highly crosslinked UHMWPE, Biomaterials, 2004, pp. 2171–2178
[15] J. S. Bergström, J.E. Bischoff, An Advanced Thermo-mechanical Constitutive Model for UHMWPE, International Journal of Structural Changes in Solids, 2010, pp. 31-39
[16] ASTM D0695-02A Test Method for Compressive Properties of Rigid Plastics.
[17] PolyUMod, A library of advanced used materials, Veryst Engineering LLC.
[18] S.R. Frost, A.M. Korsunsky, Wu Y-S, A.G. Gibson, 3-D Modeling of liner collapse. In: Conference NACE; 2000.
[19] Abaqus Analysis User´s Manual, 2010, Section 11.5.1, Dassault Systèmes, 2010.